

Ion Selectivity in Nickel Hexacyanoferrate Films on Electrode Surfaces

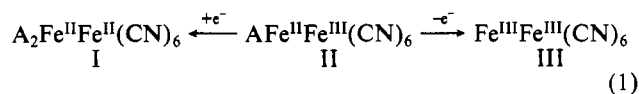
L. F. SCHNEEMEYER,* S. E. SPENGLER, and D. W. MURPHY

Received November 16, 1984

We have examined the redox behavior of anodically formed nickel hexacyanoferrate complexes on electrode surfaces. Cyclic voltammetry in dry acetonitrile solutions containing various cations indicates a clear size dependence. Li^+ and Na^+ reversibly insert into the nickel hexacyanoferrate lattice while K^+ suffers a kinetic inhibition, and larger ions are unable to insert into the lattice. This behavior is in agreement with our estimate of 0.77 Å for the size of the diffusion bottleneck. A much larger range of cation sizes are reportedly accommodated in the $\text{A}_x\text{NiFe}(\text{CN})_6$ lattice in aqueous electrolytes, and the role of water in the aqueous electrochemistry of this material is unclear. We have shown that protons (or hydronium ions) may play a role in effecting charge neutrality in these films. Sites in the cubic framework structure of nickel hexacyanoferrate, an analogue of Prussian blue, are occupied upon reduction of the film in reactions analogous to insertion or intercalation reactions, which occur for graphite or oxide framework structures.

Introduction

Electrodes modified by various metal hexacyanometalate (MHCNM) films have recently been shown to have interesting chemical and electrochemical properties. Electrochemically formed films of iron hexacyanoferrate, or Prussian blue, have been employed in electrochromic display devices.¹ The mixed-valence compound, Prussian blue (II), can be electrochemically reduced to a clear material, Everitt's salt (I), or oxidized to Berlin green (III) in processes that give well-defined cyclic voltammetric waves in aqueous solution² in accordance with eq 1. Stabilization of



the CdS semiconductor–ferrocyanide electrolyte interface is reportedly controlled by the formation of a cadmium hexacyanoferrate surface film.³ Anodization of nickel in the presence of complexes of the form $[\text{M}(\text{CN})_6]^{n-}$ ($\text{M} = \text{Fe}, \text{Ru}, \text{Mn}$) results in the formation of surface films of $\text{A}_x\text{NiM}(\text{CN})_6$ that enhance electrode stability and impart a degree of electrocatalytic activity.⁴ These nickel hexacyanometalate surfaces have been reported to undergo reactions of the type illustrated in eq 1 for all alkali metals, although the half-wave potentials and kinetics vary with the alkali metal, A .⁵

The chemistry of MHCNM films is similar to intercalation or insertion chemistry, which has been studied in a wide variety of materials, including graphite, layered transition-metal dichalcogenides, and oxides with three-dimensional framework structures.⁶ Particularly in oxide framework structures, there is a strong dependence on alkali cation size. In view of the size effects known for other materials, the range of ions reportedly accommodated, especially in the $\text{A}_x\text{NiFe}(\text{CN})_6$ film, is surprisingly large. Sizes of cation sites and diffusion pathways in these films have received limited attention, and questions as basic as the hydration state of ions as they enter the structure have not been adequately addressed. We have studied these films in dry acetonitrile solutions with various alkali-metal cations in the supporting electrolyte. Our results for the dependence of the electrochemical behavior on cation size are consistent with the known structure for nickel hexacyanoferrate.

Experimental Section

Reagent grade (ACS) sodium nitrate, potassium ferricyanide, potassium ferrocyanide, perchloric acid (Baker Chemicals), lithium nitrate, lithium perchlorate, sodium perchlorate, potassium perchlorate, potassium hexafluorophosphate, potassium tetrafluoroborate, rubidium perchlorate, and tetraethylammonium tetrafluoroborate (Alfa) were used without further purification. Water was purified in a Gelman Water I ultrapurification system. Acetonitrile was distilled from P_2O_5 .

One-compartment glass cells were used for electrochemical experiments. A Fisher saturated calomel electrode (SCE) with a porous ceramic frit served as the reference electrode for aqueous experiments. For acetonitrile studies, a Ag/0.1 M $\text{AgNO}_3/0.1$ M $\text{Et}_4\text{NClO}_4/\text{CH}_3\text{CN}$ electrode used with a Luggin capillary served as the reference electrode. The capillary tip was placed ca. 1 mm from the surface of the working electrode. The counter electrode in all experiments was platinum foil with several square centimeters of surface area. Nonaqueous experiments were carried out in a nitrogen-atmosphere Vacuum Atmospheres drybox. Electrochemical experiments were performed with a Princeton Applied Research (PAR) Model 173 potentiostat/galvanostat equipped with a Model 179 digital coulometer and a Model 175 programmer. Data were recorded on an HP Model 7044B X-Y recorder. Surface coverages were determined from the area under cyclic voltammetric waves.

Procedure for Film Formation

Two types of electrodes were used in these studies. For the first type, Ni foil contacted to a copper lead was masked with clear epoxy (Epoxy-Patch, Dexter Corp.) leaving a 1-cm² exposed disk. The nickel was polished with fine alumina sandpaper prior to anodization. For the second type of electrode, a layer of nickel was electrodeposited on a 1-cm² platinum-disk electrode with a modified Watts bath (225 g/L $\text{NiSO}_4 \cdot 6\text{H}_2\text{O}$, 60 g/L $\text{NiCl}_2 \cdot 6\text{H}_2\text{O}$, 37.5 g/L H_3BO_3 , pH adjusted with H_2SO_4 ,²⁻⁴) which was then mounted as the nickel electrode described above. For both types of electrodes, the nickel surface was then anodized in a 10 mM ferrocyanide solution with sodium nitrate as the supporting electrolyte. Anodization was carried out under potentiostatic control at 1 V vs. SCE for 1 min. The nickel on the platinum is entirely converted to the hexacyanoferrate complex while a comparable film (1.25×10^{-8} mol/cm²) is formed on the nickel. Films were dried in vacuo at 100 °C prior to nonaqueous experiments. Cyclic voltammetry of films in aqueous 0.2 M NaNO_3 solution before and after drying showed no changes in surface coverage or characteristics of the cyclic voltammetric waves.

Results and Discussion

When nickel is anodized in the presence of $\text{Fe}(\text{CN})_6^{3-}$, an insoluble nickel hexacyanoferrate complex, $\text{A}_x\text{NiFe}(\text{CN})_6 \cdot n\text{H}_2\text{O}$ ($\text{A} = \text{alkali-metal cation}$) forms as a surface film. Nickel hexacyanoferrate is an analogue of the classic mixed-valence complex Prussian blue and has the same cubic framework structure in which metal atoms are linked by cyanide units.^{7,8} This structure is shown in Figure 1. Iron and nickel atoms alternate at cube corners. The cyano groups are oriented such that all irons are coordinated exclusively to carbon and all nickels to nitrogen. The sites at the cube center, indicated by A, are occupied by alkali-

- (1) Itaya, K.; Shibayama, K.; Akahoshi, H.; Tushima, S. *J. Appl. Phys.* **1982**, *53*, 804.
- (2) (a) Neff, V. D. *J. Electrochem. Soc.* **1978**, *125*, 886. (b) Ellis, D.; Eckhoff, M.; Neff, V. D. *J. Phys. Chem.* **1981**, *85*, 1225.
- (3) Rubin, H. -D.; Humphrey, B. D.; Bocarsly, A. B. *Nature (London)* **1984**, *308*, 339.
- (4) Bocarsly, A. B.; Sinha, S. J. *Electroanal. Chem. Interfacial Electrochem.* **1982**, *137*, 157.
- (5) (a) Bocarsly, A. B.; Sinha, S. J. *Electroanal. Chem. Interfacial Electrochem.* **1982**, *140*, 167. (b) Sinha, S.; Humphrey, B. D.; Bocarsly, A. B. *Inorg. Chem.* **1984**, *23*, 203.
- (6) For a series of reviews see: Whittingham, M. S.; Jacobsen, A. J., Eds. "Intercalation Chemistry"; Academic Press: New York, 1982.

- (7) Buser, H. J.; Schwarzenback, D.; Petter, W.; Ludi, A. *Inorg. Chem.* **1977**, *11*, 1704.
- (8) Seifer, G. B. *Russ. J. Inorg. Chem. (Engl. Transl.)* **1962**, *7*, 621.

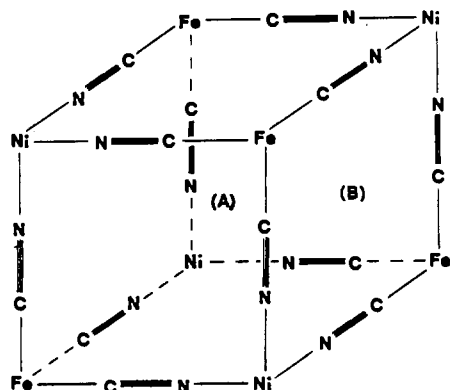


Figure 1. Structure of nickel hexacyanoferrate: (A) the site at the cube center; (B) the bottleneck at a cube face.

metal cations as necessary to achieve charge neutrality in the film. This occupancy changes with the redox state of the film, and a net diffusion of ions in and out of the film is necessary for redox reactions to occur.

To enter or vacate site A at the cube center, an ion must pass through the square opening or hole in the cube face, B. To discuss the motion of ions through B and their occupancy of A, we must estimate the sizes of these sites. From the known lattice parameter for cubic $A_x\text{NiFe}(\text{CN})_6$ and the covalent radii of Fe, Ni, C, and N, Seifer has estimated the diameter of B as 3.2 Å.⁸ This value has been quoted by several authors as being about the right size for hydrated alkali-metal ions. However, our estimate of B is much smaller. The critical term in the calculation is the estimate of the lateral radius of the cylindrical cyanide ion. Seifer took this simply as an average of the covalent radii of C and N (0.77 and 0.74 Å, respectively). We believe a more realistic value for the lateral radius of the cyanide ion is obtained from crystal structures of NaCN. Two crystal structures are known for NaCN. The room-temperature structure is of the NaCl type with freely rotating CN^- groups and a Na-CN distance of 2.94 Å.⁹ However, below 288 K, NaCN is observed to form a distorted structure having chains of Na bonded edge on to cyanide ions at a distance of 2.80 Å.¹⁰ Subtracting the ionic radius of Na^+ from each of these distances gives 3.99×3.71 Å as measures of the length and diameter of a cylindrical CN^- ion. This ionic size overestimates the known unit cell of the $A_x\text{NiFe}(\text{CN})_6$ framework ($a = 2(r_{\text{Ni}^{2+}} + r_{\text{Fe}^{3+}} + 3.99)$ 10.70 Å) by 0.70 Å, which is not unreasonable in view of the increased covalent character over NaCN. Scaling both CN^- dimensions by an appropriate factor to give the known $A_x\text{NiFe}(\text{CN})_6$ lattice constant, we obtain 3.47 Å as the lateral diameter of the CN^- link and 0.77 Å as the radius of the bottleneck, B. Using the above set of assumptions, we similarly estimate the radius of site A as 1.80 Å. These calculations indicate an A site preference of $\text{Cs} > \text{Rb} > \text{K} \gg \text{Na}$, and for B, $\text{Li} > \text{Ni} \gg \text{K}$. Neither site appears to be large enough to accommodate fully hydrated ions. These hard-sphere estimates are undoubtedly overly pessimistic especially in the case of a transition state for a polarizable ion.

Bocarsly et al. have shown that aqueous electrolytes of all the alkali metals support appreciable rates of charge transfer for nickel hexacyanoferrate films.⁵ They find that the redox potential of the surface-confined film varies with the alkali-metal cation present in the solution. The average of the potentials of the anodic and cathodic peaks, $((E_{\text{pA}} + E_{\text{pC}})/2)$, shifts monotonically with atomic number by 600 mV from Li^+ to Cs^+ . They presented an analysis of the shapes of the cyclic voltammograms, assuming hydrated cations with hydrated Li^+ larger than Cs^+ ,¹¹ responsible for effecting charge neutrality in the oxidized film and report relatively

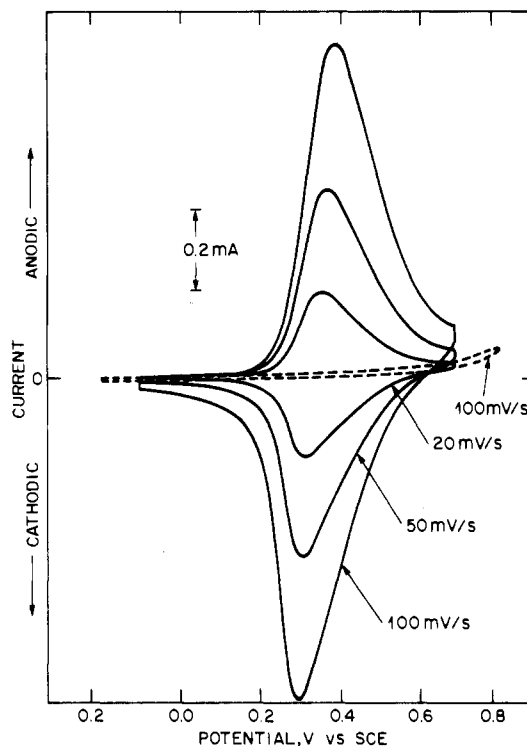


Figure 2. Cyclic voltammograms for a nickel hexacyanoferrate film on nickel in 0.2 M NaNO_3 . The dotted curve shows a nickel surface in the same electrolyte.

faster substitutional kinetics for Cs^+ and Li^+ . Other transition-metal hexacyanoferrates are reported to show much stronger cation dependences. The cation preference for Prussian blue films is, in aqueous electrolytes, $\text{K}^+ > \text{Na}^+ \gg \text{Li}^+$,^{2b,12} and copper hexacyanoferrate is reported to be K^+ specific with Na^+ blocking charge transfer.¹³ Also, Prussian blue modified electrodes were recently reported to show a cation selectivity $\text{K}^+ > \text{Na}^+ > \text{Li}^+$ in dry propylene carbonate.¹⁴

With slight adjustments to the size considerations presented above, the Prussian blue and copper hexacyanoferrate results can be explained on the basis of sizes of *unhydrated* ions. The results for nickel hexacyanometalate films are more puzzling. We have verified the experimental results of Bocarsly et al. in aqueous electrolytes. Figure 2 shows the cyclic voltammetric waves for a typical film cycled in aqueous solution with 0.1 M NaNO_3 as the supporting electrolyte. Surface coverages were determined by measuring the area under cyclic voltammetric waves. Films on nickel and platinum substrates behaved the same.

Another possible species that could be involved in insertion are protons (or hydronium ions). We have examined the electrochemistry of nickel hexacyanoferrate in acid. Prussian blue and other metal hexacyanometalates are soluble in strong acid. We observed only slow degradation of the nickel hexacyanoferrate film in dilute perchloric acid. Cyclic voltammetric waves for nickel hexacyanoferrate in 0.1 M HClO_4 are shown in Figure 3. Peaks used in acetonitrile were broadened, but appreciable charge-transfer rates are supported in the acid electrolyte. The results show that protons can play a role in the electrochemistry of these films in aqueous media.

Questions about the role of protons and the state of hydration of the alkali-metal ions have led us to examine the electrochemistry of nickel hexacyanoferrate films in acetonitrile electrolytes. Films used in acetonitrile were formed by anodization of nickel surfaces in aqueous $\text{NaNO}_3/\text{K}_3\text{Fe}(\text{CN})_6$ solutions and were dried before use. The cyclic voltammetric waves recorded in aqueous NaNO_3 electrolyte for a given film after study in acetonitrile suggest that

(9) Rowe, J. M.; Hinks, D. G.; Price, D. L.; Susman, S.; Rush, J. J. *J. Chem. Phys.* **1973**, *58*, 2039.

(10) Verweel, H. J.; Bijvoet, J. M. Z. *Kristallogr., Kristallgeom., Kristallphys., Kristallchem.* **1938**, *100*, 201.

(11) Moelwyn-Hughes, E. A. "Physical Chemistry"; Macmillan Co.: New York, 1951; p 589.

(12) Crumbliss, A. L.; Lugg, P. S.; Patel, D. L.; Morosoff, N. *Inorg. Chem.* **1983**, *22*, 341.

(13) Siperko, L. M.; Kuwana, T. *J. Electrochem. Soc.* **1983**, *130*, 396.

(14) Crumbliss, A. L.; Lugg, P. S.; Morosoff, N. *Inorg. Chem.* **1984**, *23*, 4701.

Table I. Potentials of Anodic and Cathodic Peaks in Aqueous and Acetonitrile Solutions and Ionic Radii for Various Alkali-Metal Cations

cation	ionic radius, Å	aqueous (V vs. SCE)			CH ₃ CN (V vs. Ag ⁰ /Ag ⁺) ^a		
		E_{PA}	E_{PC}	$(E_{PA} + E_{PC})/2$	E_{PA}	E_{PC}	$(E_{PA} + E_{PC})/2$
Li ⁺	0.68	0.324	0.186	0.255	0.222	0.078	0.15
Na ⁺	0.97	0.364	0.306	0.335	0.316	0.214	0.265
K ⁺	1.33	0.492	0.462	0.477	0.426	0.112	~0.3
Rb ⁺	1.47	0.642	0.528	0.585			

^a0 V vs. Ag⁰/Ag⁺ = -0.33 V vs. SCE.

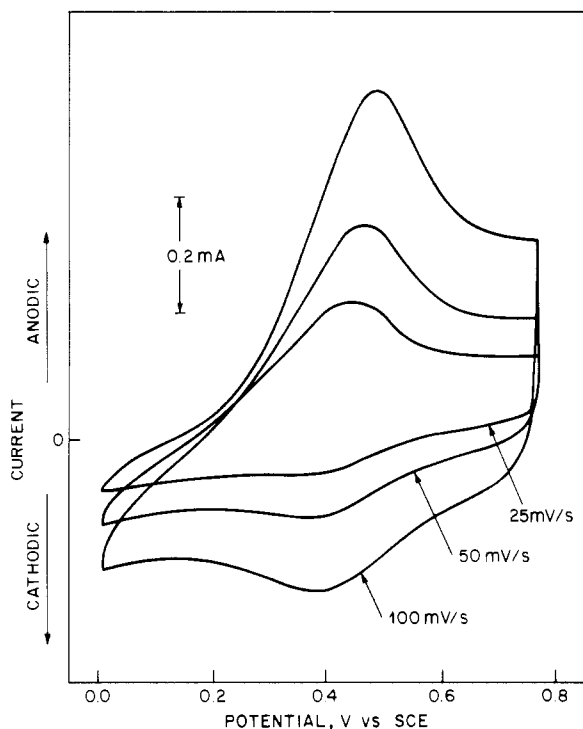


Figure 3. Cyclic voltammograms for a nickel hexacyanoferrate film in 0.1 M HClO₄.

any changes undergone by the film are reversible. The Luggin capillary minimized the effects of higher resistances in acetonitrile solutions. Well-defined cyclic voltammograms are observed for both the lithium and sodium electrolytes (Figure 4a,b). Peak currents are linear with scan rate, and the area under the cyclic voltammetric waves agrees with that of a given film cycled in aqueous sodium nitrate solution. A shift in $(E_{PA} + E_{PC})/2$ similar to that measured in aqueous solution is seen in going from Li⁺ to Na⁺ in the supporting electrolyte. However, quite different behavior is seen with K⁺ electrolytes (Figure 4c). Much more irreversibility is observed in the K⁺ waves, with broad and ill-defined oxidation peaks. The definition of reduction peaks indicates that results are not merely due to solution resistance. If the cation in the supporting electrolyte is too large to penetrate the lattice, then charge transfer should not be observed. Rb⁺ (Figure 4d) and *n*-tetraethylammonium (TEA⁺) (Figure 4e) ions are unable to support appreciable charge-transfer rates. The rise in oxidation current at the anodic limit is apparently due to a reaction of the nickel substrate as shown in Figure 4f.

These results in acetonitrile indicate a clear size dependence, which is in agreement with our estimate of the size of the diffusion bottleneck. The smallest alkali-metal cations, Li⁺ and Na⁺, reversibly insert into the nickel hexacyanoferrate lattice. For K⁺, there is a kinetic inhibition, while larger ions are unable to insert into the nickel hexacyanoferrate lattice. E_{PA} , E_{PC} , and $(E_{PA} + E_{PC})/2$ values in aqueous and acetonitrile solutions and ionic radii for the alkali-metal cations are included in Table I.

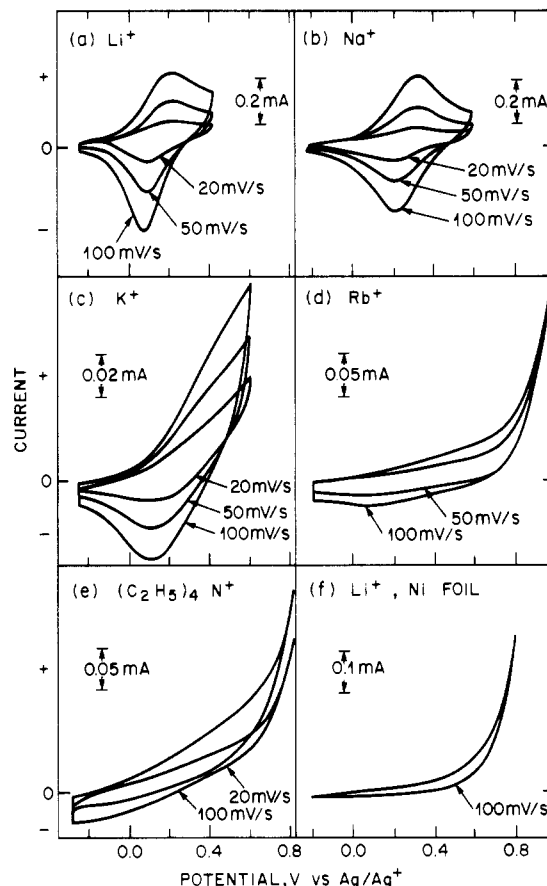


Figure 4. Cyclic voltammograms for nickel hexacyanoferrate films in acetonitrile solutions containing (a) 0.2 M LiClO₄, (b) 0.2 M NaClO₄, (c) 0.2 M KClO₄, (d) 0.1 M RbClO₄, and (e) 0.1 M *n*-Et₄NClO₄. A cyclic voltammetric curve (f) for Ni foil in acetonitrile solution containing 0.1 M LiClO₄ is also shown.

While a clear cation size dependence is observed for nickel hexacyanoferrate in nonaqueous media, no such size dependence is observed in the aqueous electrochemistry of nickel hexacyanoferrate films. The role of water in the aqueous electrochemistry of these films is unclear. Water may alter the structure of the film, allowing access to larger cations. Protons may play a role in effecting charge neutrality, particularly when other ions in solution are too large to enter the structure. Additional experiments will be necessary to elaborate the role of water in the structure and electrochemistry of this material.

Acknowledgment. We thank S. M. Zahurak for technical assistance and acknowledge helpful discussions with B. Miller and S. Sinha.

Registry No. Li, 7439-93-2; Na, 7440-23-5; K, 7440-09-7; Rb, 7440-17-7; LiClO₄, 7791-03-9; NaClO₄, 7601-89-0; KClO₄, 7778-74-7; RbClO₄, 13510-42-4; Et₄NClO₄, 2567-83-1; Ni, 7440-02-0; HClO₄, 7601-90-3; Fe(CN)₆³⁻, 13408-62-3; nickel hexacyanoferrate complex, 97644-49-0.